

Random Error Propagation Analysis in Center of Pressure Signal*

Andrew Skiadopoulos¹ and Kostas Gianikellis²

Abstract—The force measurement system unavoidably introduces noise in the output signals. The noise in the center of pressure (COP) signal is the propagation noise arise from the combination of the components used to compute it. A framework to analyze the random error in COP signals was introduced based on the “Guide to the Expression of Uncertainty of Measurement” (GUM) approach. Furthermore, the spatiotemporal resolution criterion was used as a parameter to evaluate force measurements systems under specific experimental conditions.

I. INTRODUCTION

A strain gauge force platform is a robust and accurate easy-to-use force measurement device that is typically composed of four load cells each one bonded with electric resistance stain gauges that produce a resistance change that varies linearly with strain and which convert the magnitude of the local stretching of gauge into an electrical signal proportional to the magnitude of force that they experience. The output electrical signal from the transducers is usually processed by passing through a signal conditioner, which performs tasks such as amplification and analog filtering of unwanted frequencies, and then it is recorded using a data acquisition system, calibrated, filtered digitally and stored for further off-line processing. The four load cells register the applied forces along each of the anterior-posterior (X), medial-lateral (Y) and vertical (Z) axes of platform’s orthogonal reference system. Individual reaction forces are measured by the three components of each of the four load cells and the temporal evolution of the force components, F_x , F_y and F_z of the ground reaction forces (GRF) is determined. The coordinates of the point where the resultant of the GRF components intersects the support surface (center of pressure, COP) at every instant are calculated as a function f of the components of the GRF measured by each load cell [1-6].

The force measurement system unavoidably introduces noise in the output signals. The noise in the COP signal is the propagation noise arise from the combination of the components used to compute it with function f . Generally, it is modeled as a wide-band additive, stationary, zero-mean, and uncorrelated noise that contaminates the low-pass COP signal with noise variance σ^2 . However, even if the noise of the recorded GRF signals can be modelled as an additive zero-mean “white noise”, the nonlinear transformation in

COP computation destroys these properties to some extent [7]. The noise in the COP signal becomes nonstationary (i.e., unequal noise variance), except for the case where the F_z is constant. Noise stationarity may be true for stabilometric studies [8] and digital low-pass filter or smoothing techniques can be used to remove high frequencies presented in the COP signal [9]. The optimal cut-off frequency for the low-pass digital filter can be found by residual analysis [10] or by using the generalized, crossed-validators natural splines smoothing algorithm (GCVSPL) [9]. Natural splines of m^{th} order behave like an m^{th} order double Butterworth filter, where optimal cut-off frequency is the lowest frequency for which the residual noise is white [11].

Moreover, with sufficient *oversampling* is possible to retain significant signal components avoiding aliasing errors, while reducing noise level [12]. The noise variance presented in a signal, or in its derivatives, after optimal smoothing depends on the bandlimit of the signal and is proportional to the sampling rate and the variance of the inherent band-limited “white noise” presented in the raw data measurement [13], and is expressed as

$$\sigma_k^2 = \sigma^2 \tau \frac{\omega_b^{2k+1}}{\pi(2k+1)} \quad (1)$$

where

- σ_k^2 is the noise variance in the estimate k^{th} order derivative
- σ^2 is the noise variance in the raw measured data (additive “white noise”)
- τ is the sampling interval ($\tau = \frac{1}{f_s} = \frac{1}{2\pi\omega_0}$ with $\omega_0 \geq 2\omega_b$)
- ω_b is the bandlimit of the signal
- k is the order of the derivative

The term $\sigma^2 \tau$ is known as spatiotemporal resolution criterion (Q_{ST}) and together with Shannon’s sampling theorem can be regarded as sufficient criteria in order to choose the sampling frequency ω_0 [7, 12, 14, 15]. When a quantizing data acquisition system with sampling frequency ω_0 introduces sampling “white noise” with variance σ^2 , oversampling would result in its reduction [12]. Therefore, the sampling rate must not violate Shannon’s sampling theorem in order to avoid aliasing, but it can be much greater than twice the ω_b in order to reduce the amount of noise mapped into the Nyquist band, as long as the measurement noise above a chosen Nyquist frequency is white [7, 12, 14, 15]. Since physical signals are not strictly bandlimited and therefore ω_b is unknown [16], the cross-over frequency ($\omega_c = 2\pi f_c$) beyond which the noise level is dominant can be used instead, as long as it is not less than the signal bandlimit ($\omega_c \geq \omega_b$) [7, 10, 13, 14, 17]. Once more, sampling

*This work was not supported by any organization

¹Andrew Skiadopoulos is with Biomechanics of Human Movement and Ergonomics Lab., Universidad de Extremadura, Cáceres, Spain andreas@unex.es

²Kostas Gianikellis is with the Biomechanics of Human Movement and Ergonomics Lab., Universidad de Extremadura, Cáceres, Spain kgiannik@unex.es

frequency greater than twice the ω_c can be used as long as the noise above the Nyquist frequency is white. In any case, the sampling rate should not be more than

$$\tau_{max} = \frac{\sigma_k^2 \pi(2k+1)}{\sigma^2 \omega_b^{(2k+1)}}$$

for a required precision σ_k^2 [13].

The Q_{ST} has been used as a figure of merit to evaluate motion capture systems [7, 12, 14, 15]. However, is a figure of merit for any noisy sampled data system [12, 14, 15] that deals with zero-mean “white noise” introduced by the data acquisition system. Small values of Q_{ST} corresponds to less system’s noise. Assuming a perfect input signal, Q_{ST} corresponds with the power spectral density of the quantization error [18]. By increasing the sampling rate the quantization noise power spreads over a larger frequency band improving the quality of the signal that is smoothed by a digital low-passed post-filter. Oversampling improves the precision of the measurement by increase the resolution of the quantizer, however, only for a bit for every quadruplicate of the Nyquist frequency. When a differential quantization it is considered, the quantization error added in the reconstructed quantized signal is even less, but the sampling frequency has to be significantly higher than the Nyquist frequency [14, 18, 19]. On the other hand, by increasing sampling frequency when a signal is varying slowly the noise will not be any more white [13, 14]. Moreover, by increasing sampling frequency it is also increased the bandwidth of the preceding analog system which may increase the noise superimposed on the input signal to no optimal values. A tradeoff exist between oversampling and signal’s noise variance, however, this is equipment related [7]. By increasing the sampling rate of the force measurement system it has been showed that the COP noise increases [20].

A. Influence of force magnitude on COP

In many other fields of biomechanical studies, there are instants where the applied vertical component of the GRF vector (\mathbf{F}_z) changes its magnitude drastically during its evolution in time (Figure 1). These fluctuations in \mathbf{F}_z between the “load-unload” phases, result in variations in noise variance presented in the raw COP coordinates. It has been shown experimentally that a decrease in \mathbf{F}_z corresponds to an increase in noise variance related by a fractional quadratic function [21]. Accordingly, in those experimental situations where \mathbf{F}_z changes drastically, the noise presented in the raw COP coordinates could be modeled as additive, zero-mean, and nonstationary–i.e., unequal noise variance across COP coordinates and variations in time of the noise power. Weak-correlated noise is also assumed. This renders time-invariant Fourier transform based filtering techniques or GCVSPL suboptimal.

By assuming that the noise is zero-mean “white noise” and additive to the COP signal, the quality of COP signal and of its derivatives after optimal smoothing or filtering depends on the proportion of the noise variance that lies inside the

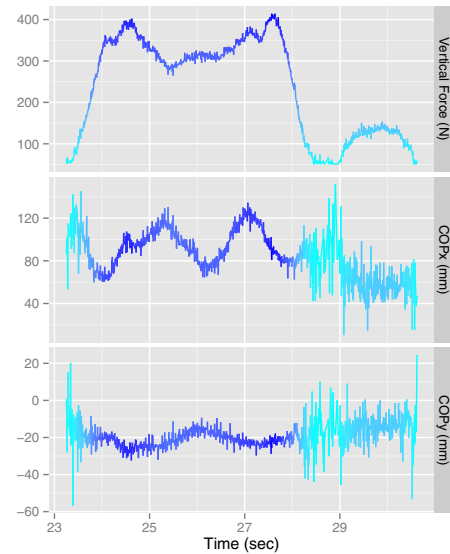


Fig. 1. In asymmetric lifting or lowering tasks in the ergonomics context, there are intervals where the magnitude of the F_z obtained by the force measurement system fluctuates. Clearly, there are intervals where F_z changes its magnitude drastically. These fluctuations result in variations in the variance presented in the raw COP coordinates (COPx-anterio-posterior; COPy-mediolateral)

bandlimit of the signal after oversampling rate had spread it evenly over the Nyquist interval [13, 17]. However, when the noise is nonstationary, low-pass filtering is not an adequate option as it imposes the same cut-off frequency for the entire signal. Moreover, in dynamic tasks, portions of COP signal may contains high-frequency components. An optimal solution is smoothing or low-pass filtering the raw signals of the components upon COP depends before its computation, however, this is not always possible. Another solution is to use adaptive Fourier transform based [22] or time-frequency filters [23, 24, 25, 26]. However, optimal cut-off frequency is difficult to obtain. Another solution is to construct a weighted matrix of the associated noise variance in the COP signal and smooth using the GCVSPL package under mode 1, by using the mean square error at each COP point [9]. However, knowledge of the noise variance is needed previously.

Therefore, the aim of this study was to analyze the noise in the COP signal under different experimental conditions and in turns to construct a weighted variance matrix for the COP noise in conformance with the GUM approach [27]. In Part II, the theoretical model of the propagation error in the COP resulted from the combination of the components used to computed it is presented step-by-step, whereas in Part III the proposed approach is demonstrated experimentally, where some noise curves are presented.

II. APPLICATION OF THE LAW OF PROPAGATION OF UNCERTAINTIES

A. General Uncertainty Framework

Consider a single real output quantity Y that is related to a vector of real input quantities $\mathbf{X} = (X_1, \dots, X_N)^T$ by an explicit univariate measurement model $Y = f(\mathbf{X})$. The esti-

mate of the output quantity is $y = f(\mathbf{x})$ with $\mathbf{x} = (x_1, \dots, x_N)$. Assuming linear or weakly-nonlinear relation and using a first-order Taylor series expansion, the standard uncertainty u_y associated with y is obtained by the “law of propagation of uncertainties” expressed by

$$u_y^2 = S_x \mathbf{U}_x S_x^T \quad (2)$$

where S_x is the vector of the sensitivity coefficients expressed by the values of the partial derivatives $\frac{\partial f}{\partial x_j}$ for $j = 1, \dots, N$, at $\mathbf{X} = \mathbf{x}$ and \mathbf{U}_x is the $N \times N$ uncertainty matrix associated with \mathbf{x} containing the covariances $u(x_i, x_j)$ for $i, j = 1, \dots, N$ associated with x_i and x_j .

B. Uncertainty estimation in COP signal

1) *Measurement Model*: The objective is to estimate the uncertainty in the COP measurand. The estimate of the input quantities upon COP is computed and the associate uncertainty matrix U_x are propagated through a linearization of the measurement model that relates the measurand with the input quantities

$$COP = f(x_1, \dots, x_N)$$

2) *Measurement Function*: The COP location in the X axis was calculated using the measurement function

$$COP = \frac{M_x}{F_z} \quad (3)$$

where $M_x = (F_z^3 + F_z^4)L$ is the magnitude of the moment of force and L is the constant distance factor (with no uncertainty), $F_z = F_z^1 + F_z^2 + F_z^3 + F_z^4$ is the magnitude of the vertical component of the GRF vector, and F_z^1 to F_z^4 are the magnitudes of the vertical components of the GRF vector measured by each load cell. In terms of the GUM annotations

$$COP \equiv f(F_z^1, F_z^2, F_z^3, F_z^4, L)$$

3) *Error Model*: It is assumed that (3) is continuous and it has also continuous derivatives in the domain of interest. The error model is determined from (3) by applying a first-order Taylor series approximation. The COP error equation is expressed as

$$\varepsilon_y = S_x \varepsilon_x^T$$

where S_x is the sensitivity vector assuming that L has no associated uncertainty

$$S_x = \left[\frac{\partial COP}{\partial F_z^1} \quad \frac{\partial COP}{\partial F_z^2} \quad \frac{\partial COP}{\partial F_z^3} \quad \frac{\partial COP}{\partial F_z^4} \right]$$

and ε_x is the error vector associated with the inputs quantities

$$\varepsilon_x = \left[\varepsilon_{F_z^1} \quad \varepsilon_{F_z^2} \quad \varepsilon_{F_z^3} \quad \varepsilon_{F_z^4} \right]$$

4) *Uncertainty Model*: The associated u_y^2 in the COP measurements is the variance in the propagated error resulted from the combination of the components used to compute COP. Therefore, if $u_{F_z^1}^2$ to $u_{F_z^4}^2$ are the noise variances of the F_z^1 to F_z^2 components respectively, the uncertainty in COP measurement is then expressed by (2) where \mathbf{U}_x is the 4×4 symmetric uncertainty — variance-covariance — matrix associated with \mathbf{x}

$$\mathbf{U}_x = \begin{bmatrix} u^2(F_z^1) & u(F_z^1, F_z^2) & u(F_z^1, F_z^3) & u(F_z^1, F_z^4) \\ u(F_z^2, F_z^1) & u^2(F_z^2) & u(F_z^2, F_z^3) & u(F_z^2, F_z^4) \\ u(F_z^3, F_z^1) & u(F_z^3, F_z^2) & u^2(F_z^3) & u(F_z^3, F_z^4) \\ u(F_z^4, F_z^1) & u(F_z^4, F_z^2) & u(F_z^4, F_z^3) & u^2(F_z^4) \end{bmatrix}$$

The diagonal terms of \mathbf{U}_x are the uncertainty (variance) of the input quantities and the off-diagonal terms are their mutual uncertainties (covariance).

5) Measurement Process Errors:

a) *Identification*: It is assumed that the F_z^1 to F_z^4 signals are interfered with zero-mean band-limited “white noise”. The assumed error variance sources are the quantization error of the A/D card, the “white noise” inherent to the analog signal input and any additional random error that may be arose while recording and during data analysis originated by degradation of the equipment over time from previous usage or user abuse, or from influences of installation and operation environment.

b) *Estimation*: Since the error components were assumed to follow a normal probability distribution, the uncertainty in the input quantities is estimated by the standard deviation of the sample data. It was assumed that the noise variances of the signals registered by each load cell are equals ($u_{F_z^1}^2 = u_{F_z^2}^2 = u_{F_z^3}^2 = u_{F_z^4}^2$) and their sum equals the variance obtained by the force measurements system ($u_{F_z^1}^2 + u_{F_z^2}^2 + u_{F_z^3}^2 + u_{F_z^4}^2 = u_{F_z}^2$) for a static registration—i.e., $u_{F_z^{1 \rightarrow 4}} = \frac{u_{F_z}}{4}$. Furthermore, a high negative correlation coefficient was assumed between the errors in the input quantities ($\rho = -0.9$) since $F_z^{1 \rightarrow 4}$ tend to vary in opposite directions when the same F_z is displaced. Hence, the noise standard uncertainty in COP measurement is

$$u_y = \frac{1}{2\sqrt{5}F_z^2} L \left(\left((F_z^1)^2 + (F_z^2)^2 + 36F_z^2(F_z^3 + F_z^4) + (F_z^3 + F_z^4)^2 + 2F_z^1(F_z^2 + 18(F_z^3 + F_z^4)) \right) u^2 \right)^{-\frac{1}{2}}$$

6) *Mathematical optimization*: The method of Lagrange multipliers was used to find the minimum value of the standard uncertainty u_y subject to the constraint $F_z = F_z^1 + F_z^2 + F_z^3 + F_z^4$ ($F_z^{1 \rightarrow 4}, u_z \in R_{\geq 0}$). This yields

$$\min \{u_y\} = L \frac{u_z}{2\sqrt{5}F_z}, \text{ for } F_{1z \rightarrow 4z} = \frac{F_z}{4} \quad (4)$$

TABLE I
TECHNICAL CHARACTERISTICS AND CONDITIONS OF THE FORCE
MEASUREMENT SYSTEM

Sensors	OCTEC-IBV
Lowest recommended vertical force	250 N
Deadband	50 N
Maximal vertical force	15 kN
Maximal shear force	7.5 kN
Maximal force error	< 2%
Cross-talk sensitivity	Null due to mechanic
Maximal error about the COP	± 2 mm
Maximal sampling rate	1000 Hz/platform
Maximal registry time at 1000 Hz	16 sec
A/D converter	CIO-AD-16Jr, 12 bits, differential quantization
Outcome variables	GRF, M, J, COP
Top plate	CELTEC-IBV
Natural frequency of the top plate	> 400 Hz
Mounting	Concrete slab

C. Noise uncertainty in COP after Optimum Smoothing

According to (1) the noise standard uncertainty of the COP signal after optimal smoothing is

$$u_o \geq \frac{Lu_z}{F_z} \sqrt{\frac{\tau f_b}{10}} \quad \text{by (4)}$$

III. EXPERIMENTAL SETUP

A. Material

Two strain-gauge force platforms (Dinascan 600M, IBV, Valencia, Spain) were utilized to obtain the temporal evaluation of the components of the GRF vector and the coordinates of the COP during the experiment at sampling rate of 30 Hz. Table (I) shows the characteristics of the force platform system according to the manufacturer. Calibrated dead loads (Telju, Spain) was used.

B. Test setup

The force measurement system was switched on always 15 min prior to the measurement process to reach thermal stability. A calibrated dead load (M) was displaced on the top plate of the force platform from the point P_0 to the point P_{10} gradually in 10 consecutive stages that corresponded to 11 fixed points and then was returned back from the point P_{10} to the point P_0 in a similar manner. This operation was repeated two times. During the displacements of the dead load M from the point P_0 to the point P_{10} and back to the P_0 , at each one of the intermediate points where the load M was placed gradually, the COP was measured for 10 repeated times in an interval of 30 sec between each repetition. Each repeated COP data was collected for a time period of 5 sec at sampling rate of 30 Hz under a set of repeatability conditions of measurement. By the help of a millimetre grid that was placed on the top plate of the force platform, the distance between each consecutive point was fixed at 10 mm. Therefore, the measurement range was set at 100 mm. Furthermore, all the points were laying on a line which is parallel to the X- or Y-axis and crosses the

geometrical center of the top plate of the force platform. Moreover, all the points were contained within the area ± 50 mm from the geometrical center of the top plate of the force platform in both the X- and Y-axis. To ensure that the load M was placed with accuracy onto the fixed points on the grid, a point loader was used. The force platform was zeroed only at the begin of the procedure. The same operator conducted the whole procedure. This procedure was repeated for different calibrated loads (range: from ≈ 98 N to ≈ 294 N) for the two force platforms used in the study.

In addition, a dead load (≈ 294 N) was placed on the top plate of the force platform about its geometrical center and the COP was registered at 30, 230 and 500 Hz for 10 sec. A frequency analysis was made on the COP signals to test whether COP noise is “white”. To test the influence of the sampling rate another dead load (≈ 294 N) was placed on the top plate of the force platform about its geometrical center and the COP was registered for 10 sec at an integer sequence of frequencies (30, 40, 50, ..., 300 Hz).

1) *Point Loader Specifications*: To ensure that dead loads have been placed accurately on the co-ordinates indicated by the millimetre grid, the dead load M was placed on a metallic platen that in turns was placed above two parallel adjustable metal bars sustained on the ground away from the force platform being evaluated. A stylus of 5 mm diameter was stuck to the surface of the platen at its geometrical center in order to transmit the load on the top plate of the force platform.

Any bias associated with the grid and dead load and the comparison procedure were considered irrelevant to the procedure.

C. Data Processing and Analysis

There are $k = 10$ repeated COP samples comprised of 150 data each, for each one of the 11 fixed points $P_{0 \rightarrow 10}$, replicated $r = 4$ times. For each point the mean value and standard deviation for each repeated COP sample have been computed, as well as the overall mean value comprised of all the data of the $k = 10$ repeated samples. The overall mean (\bar{y}) and its standard deviation (s) have been computed by

$$\bar{y}_i = \frac{1}{n_i} \sum_{j=1}^{n_i} y_{ij}$$

and

$$s_i = \sqrt{\frac{1}{n_i - 1} \sum_{j=1}^{n_i} (y_{ij} - \bar{y}_i)^2}, \quad \text{with } i = 1, \dots, k.$$

where

- n_i = the i^{th} repeated COP sample size
- \bar{y}_i = mean value for the i^{th} repeated COP sample
- s_i = standard deviation of i^{th} repeated COP sample
- y_{ij} = the j datum of the i^{th} repeated COP sample.

TABLE II
RESULTS OF SPATIOTEMPORAL RESOLUTION CRITERION (Q_{ST})

	M_{10}	M_{20}	M_{30}
Force Platform 1 X-axis	1.017	0.427	0.278
Force Platform 1 Y-axis	0.984	0.398	0.263
Force Platform 2 X-axis	1.037	0.391	0.268
Force Platform 2 Y-axis	0.869	0.336	0.230

The overall mean value for the $k = 10$ repeated samples at each point is computed as

$$\bar{y} = \frac{1}{n} \sum_{i=1}^k \sum_{j=1}^{n_i} y_{ij} = \frac{1}{n} \sum_{i=1}^k n_i \bar{y}_i$$

where $n = \sum_{i=1}^k n_i =$ total number of measurements. In total four overall means have been calculated at each point, one for every replication. The standard deviation, s , of all repeated COP samples for one replication for each point is [28]

$$s = \sqrt{s_b^2 + s_w^2}$$

The standard deviation of the sampled mean values relative to the overall mean value is the between sample sigma, s_b , computed as

$$s_b = \sqrt{\frac{1}{n-1} \sum_{i=1}^k n_i (\bar{y}_i - \bar{y})^2}$$

and the standard deviation within samples is the within sample sigma (noise), s_w , computed as

$$s_w = \sqrt{\frac{1}{n-1} \sum_{i=1}^k (n_i - 1) s_i^2}$$

IV. RESULTS AND DISCUSSION

The results showed that for $F_z = \text{constant}$ the noise of the COP signal can be modelled as additive, zero-mean “white noise” (Fig. 2 and 3). Different sampling rates influence the COP noise. This is obvious for the COP signals that were registered with a very different (low - very high) sampling rate (Fig. 2). For example, the variances of the raw COP data for different sampling rates are $\text{RAW}_y\text{-}30\text{Hz} = 0.54 \text{ mm}^2$, $\text{RAW}_y\text{-}230\text{Hz} = 0.59 \text{ mm}^2$, $\text{RAW}_y\text{-}500\text{Hz} = 0.61 \text{ mm}^2$, and $\text{RAW}_x\text{-}30\text{Hz} = 1.10 \text{ mm}^2$, $\text{RAW}_x\text{-}230\text{Hz} = 1.20 \text{ mm}^2$, $\text{RAW}_x\text{-}500\text{Hz} = 1.30 \text{ mm}^2$ (Fig. 3). However, for a narrower frequency interval the assumption that the sampling rate do not influence the COP noise can be considered as correct. Notwithstanding, the noise elimination, was higher after oversampling spread the power over higher frequencies. The variance of the COP signals after low-pass filtering is $\text{BTW}_x\text{-}30\text{Hz} = 0.24 \text{ mm}^2$, $\text{BTW}_x\text{-}230\text{Hz} = 0.05 \text{ mm}^2$, $\text{BTW}_x\text{-}500\text{Hz} = 0.03 \text{ mm}^2$ and $\text{BTW}_y\text{-}30\text{Hz} = 0.15 \text{ mm}^2$, $\text{BTW}_y\text{-}230\text{Hz} = 0.03 \text{ mm}^2$, $\text{BTW}_y\text{-}500\text{Hz} = 0.02 \text{ mm}^2$ (Fig. 3). Other studies have also been shown that cut-off frequency and sampling rate influence stabilometric parameters [29, 30]. However, our study demonstrated that this is dependent also on the magnitude of the vertical force. Moreover, the quality of the

TABLE III
STANDARD UNCERTAINTY IN F_z (N) OBTAINED FOR DIFFERENT DEAD LOAD WEIGHTS.

	M_{10}	M_{20}	M_{30}	M_{40}
Force Platform 1	1.90	1.86	2.00	1.84
Force Platform 2	1.96	1.81	1.75	2.08

COP signal was improved when Q_{ST} decreased (Table II) by increasing F_z magnitude.

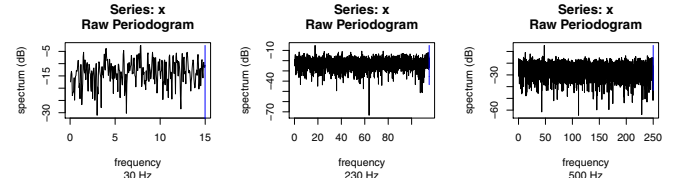


Fig. 2. Power spectral density of the raw COP signals obtained at different sampling rates (only the COPx is shown).

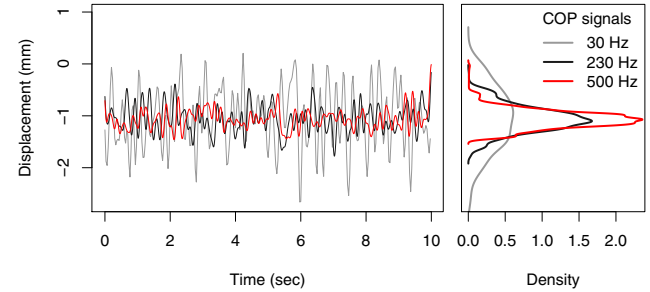


Fig. 3. COP signals with different sampling rates (30, 230 and 500 Hz) after low-pass filtering with a fourth-order zero-phase-shift Butterworth filter (BTW) with cut-off frequency at 5 Hz [1]. The probability function for the distribution is shown for each time series (only the COPx is shown).

There is not a trend among the standard uncertainty of the F_z signal registered with the different dead load weights (Table III). Therefore, the highest standard uncertainty of both force platforms, ($u_{F_z} = 2.1 \text{ N}$) was chosen (Table III). The u_y in the COP measurements is modeled as an hyperbolic function of the F_z magnitude ($u_{F_z} = c$). According to (4) the minimum u_y is obtained when the dead load is placed at the geometrical centre of the top plate of the force platform as in this point the same fraction of the F_z is registered by each load cell. Fig. (4) shows the experimental obtained noise curve together with the minima curve of the model for two cases of statistically correlated error sources, $\rho = -0.9$ and $\rho = -0.8$. The variance explained by the fitted regression models (R^2) are very high and their match with the error model is obvious. For the Y-axis the experimental obtained COP uncertainty is better modelled with statistically correlated error $\rho = -0.8$, while for the X-axis with $\rho = -0.9$.

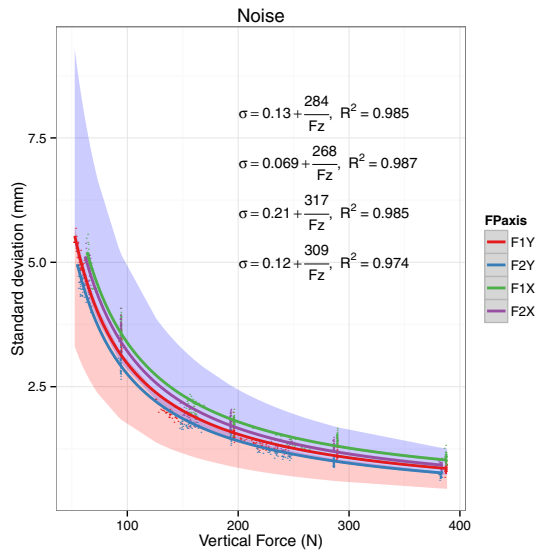


Fig. 4. Values of the u_y obtained by the “propagation law”, along with the experimentally obtained standard deviation data fitted with regression lines. The coloured areas are bounded by the values of u_y for $\rho = -0.9$ (low) and $\rho = -0.8$ (up). Blue and red areas correspond to the u_y of the X and Y axes, respectively (F1X= Force platform 1 X-axis; F1Y= Force platform 1 Y-axis; F2X= Force platform 2 X-axis; F2Y= Force platform 2 Y-axis;)

V. CONCLUSION

The implementation of the GUM approach [27] to calculate standard uncertainties for specifying the weighted factor for each coordinate of the noisy COP data was introduced. The obtained noise curves can be used (the experimental or the theoretical) in order to obtain the weighted matrix for smoothing purposes. Studies have to take into consideration how acquisition settings like sampling rate, cut-off frequency and F_z magnitude influence the COP values.

ACKNOWLEDGMENT

This manuscript has been partially supported by the Government of the Community of Extremadura, Grant Ref. GR10178.

REFERENCES

- [1] D. A. Winter, *Biomechanics and motor control of human movement*. NJ, USA: John Wiley and Sons, 2009, pp. 371.
- [2] V. Medved, *Measurement of human locomotion*. Boca Raton, FL: CRC Press, 2001, pp. 272.
- [3] R. Bartlett, *Introduction to sport biomechanics: Analysing human movement patterns*. NY, USA: Routledge, 2007, pp. 292.
- [4] A. Lee and M. Lake, “Force and pressure measurements”, in *Biomechanical evaluation of movement in sport and exercise. The British association of sport and exercise sciences guidelines*, C. J. Payton and R. M. Bartlett, Eds. Oxon, UK: Routledge, 2008, pp. 53-76.
- [5] A. Hunt, *Guide to the measurement of force*. London, UK: The Institute of Measurement and Control, 1998.
- [6] J. H. Challis, “Data processing and error estimation”, in *Biomechanical evaluation of movement in sport and exercise. The British association of sport and exercise sciences guidelines*, C. J. Payton and R. M. Bartlett, Eds. Oxon, UK: Routledge, 2008, pp. 129-152.
- [7] H. Woltring, “Smoothing and differentiation techniques applied to 3D data”, in *Three-dimensional analysis of human movement*, P. Allard, I. A. F. Stokes and J.-P. Blachi, Eds. Champaign, IL: Human Kinetics, 1995, pp. 79-99.

- [8] A. Karlsson and H. Lanshammar, Analysis of postural sway strategies using an inverted pendulum model and force plate data, *Gait and Posture*, vol. 5, pp. 198-203, June. 1997.
- [9] H. Woltring, A fortran package for generalized, cross-validated spline smoothing and differentiation, *Advances in Engineering Software*, vol. 8, pp. 104-107, Apr. 1986.
- [10] D. A. Winter and A. E. Patla, *Signal processing and lineal systems for the movement sciences*. Waterloo, Ontario, Canada: Waterloo Biomechanics, 1997, pp. 110.
- [11] H. J. Woltring, A. de Lange, J. M. G. Kauer and R. Huiskes, “Instantaneous Helical Axis Estimation Via Natural, Cross-Validated Splines”, in *Biomechanics: Basic and Applied Research. Selected Proceedings of the Fifth Meeting of the European Society of Biomechanics*, G. Bergmann, R. Klbel and A. Rohlmann, Eds. Dordrecht, GER: Martinus Nijhoff Publishers, 1986, pp. 121-128.
- [12] E. H. Furnée, Advances in tv/computer motion monitoring, in *Engineering in Medicine and Biology Society, 1989. Images of the Twenty-First Century., Proceedings of the Annual International Conference of the IEEE Engineering in*, vol. 3, pp. 1053-1054.
- [13] H. Lanshammar, On precision limits for derivatives numerically calculated from noisy data, *Journal of Biomechanics*, vol. 15, pp. 459-470, 1982.
- [14] H. Woltring, “Chapter Ib On Methodology in the Study of Human Movement”, in *Advances in Psychology. Human motor actions - Bernstein reassessed*, H. T. A. Whiting, Ed. North-holland, Dec. 1984, pp. 35-73.
- [15] E. H. Furnée, TV/computer motion analysis systems. The first two decades, Ph.D. dissertation, Applied Sciences, Delf University of Technology, Delf, The Netherlands, 1989.
- [16] D. Slepian, On bandwidth, *Proc. IEEE*, vol. 64, pp. 292-300, Mar. 1976.
- [17] H. Lanshammar, On practical evaluation of differentiation techniques for human gait analysis, *Journal of Biomechanics*, vol. 15, pp. 99-105, 1982.
- [18] S. J. Orfanidis, *Introduction to signal processing*. 2010.
- [19] J. G. Proakis and D. G. Manolakis, *Digital Signal Processing. Principles, algorithms, and applications*. Upper Saddle River, NJ, USA: Prentice-Hall, 1996, pp. 1016.
- [20] M. H. Granat, C. A. Kirkwood and B. J. Andrews, Problem with the use of total distance travelled and average speed as measures of postural sway, *Medical and Biological Engineering and Computing*, vol. 28, pp. 601-602, Nov. 1990.
- [21] D. Wisleder and B. McLean, Movement artifact in force plate measurement of postural sway, in *Proc. 2nd N. American Conf. of Biomechanics*, Chicago, 1992, pp. 413-414.
- [22] K. S. Erer, Adaptive usage of the Butterworth digital filter, *Journal of Biomechanics*, vol. 40, pp. 2934-2943, 2007.
- [23] A. Georgakis, L. K. Stergioulas and G. Giakas, Wigner filtering with smooth roll-off boundary for differentiation of noisy nonstationary signals, *Signal processing*, vol. 82, pp. 1411-1415, Oct. 2002.
- [24] G. Giakas, “Power spectrum analysis and filtering”, in *Innovative analyses of human movement*, N. Stergiou, Ed. Champaign, IL: Human Kinetics, 2004, pp. 223-258.
- [25] G. Giakas, L. K. Stergioulas and A. Vourdas, Time-frequency analysis and filtering of kinematic signals with impacts using the Wigner function: accurate estimation of the second derivative, *Journal of Biomechanics*, vol. 33, pp. 567-574, May. 2000.
- [26] J. S. Walker, *A primer on wavelets and their scientific applications*. Boca Raton, FL: Chapman and Hall/CRC, 2008, pp. 320.
- [27] JCGM 100:2008, *Evaluation of measurement data Guide to the expression of uncertainty in measurement JCGM 100:2008 (GUM 1995 with minor corrections)*, Paris: BIPM Joint Committee for Guides in Metrology, 2008.
- [28] NASA HDBK-8739, *Measuring and test equipment specifications*, Washington DC: NASA, July, 2010.
- [29] M. Schmid, S. Conforto, V. Camomila, A. Cappozzo, T. D’Alessio. The sensitivity of posturographic parameters to acquisition settings, *Medical Engineering and Physics*, Vol. 24, pp. 623-631, 2002.
- [30] F. Scoppa, R. Capra, M. Gallamini, R. Shiffer. Clinical stabilometry standardization Basic definitions - Acquisition interval - Sampling frequency. *Gait and Posture*, Vol. 37, pp. 290-292, 2013.